Mechanical Systems and Signal Processing 28 (2012) 528–541

Contents lists available at SciVerse ScienceDirect

Mechanical Systems and Signal Processing

journal homepage: www.elsevier.com/locate/ymssp

Application of magnetorheological fluid in industrial shock absorbers

Andrzej Milecki *, Mikołaj Hauke

Poznan University of Technology, 60-965 Poznan, ul. Piotrowo 3, Poland

ARTICLE INFO

Article history:
Received 26 April 2011
Received in revised form
21 October 2011
Accepted 11 November 2011
Available online 26 December 2011

Keywords:
Shock absorber
Magnetorheological fluid
Modelling

ABSTRACT

The paper presents investigation results of a semi-active industrial shock absorber with magnetorheological (MR) fluid, which is capable of controlling the stopping process of moving objects, e.g. on transportation lines. The proposed solution makes it possible to adjust the braking force (by electronic controller) to the kinetic energy of the moving object. The paper presents an overview of passive shock absorbers. Next, the design concept of a semi-active shock absorber with the MR fluid is proposed. The theoretical model and the simulation model of the MR absorber and the stopping process are presented. The paper reports investigations of a prototype MR shock absorber used to stop a mass moving on an inclined plane. The braking force of the absorber was changed by an electronic control system according to the current position of the moving mass. Finally, the simulation and investigation results are discussed and compared.

© 2011 Elsevier Ltd. All rights reserved.

1. Introduction

The gentle stopping of elements moving with high velocities on a production line is a serious problem in many industrial applications. The stopping process is usually performed by passive hydraulic shock absorbers, which protect the moving elements and other production line devices against high dynamic forces. The industrial absorbers produced today are able to ensure the gentle stopping of elements with kinetic energy in the range from 0.1 J to even 30 000 J, on braking distances from 5 mm to 400 mm. The most commonly used absorbers dissipate energy from 10 J to 80 J on distances from 20 mm to 100 mm. Leading companies producing industrial shock absorbers are ACE, Festo and ITT Enidine Inc.

Theoretically the optimal breaking process occurs when the breaking force is constant on the whole stroke of the absorber [1]. The passive shock absorbers which are in use now do not guarantee this. The braking force of these absorbers is not constant, and, as a result, the stopping process is not optimal. Therefore there is a need for improvement. Recently, semi-active devices, also called "intelligent" devices, have been proposed for the damping of vibrations and oscillations. The parameters of these devices, like the movement opposite force, can be continuously changed with minimal energy requirements. They utilise electrorheological (ER) or magnetorheological (MR) fluids. Such fluids can be quite attractive for industrial applications in the stopping of moving elements on production lines. Compared to conventional electrorheological solutions, MR devices are stronger and can be operated directly from low-voltage power supplies [2]—this is why MR fluids are much more often used.

MR fluids belong to the general class of smart materials whose rheological properties can be modified by applying a changing electric or magnetic field. These fluids have been known since the late 1940s when Winslow [3] suggested their

* Corresponding author. Tel.: +1 48 61 665 2187; fax: +1 48 61 665 2200.
E-mail addresses: andrzej.milecki@put.poznan.pl (A. Milecki), mhauke@wp.pl (M. Hauke).

0888-3270/$ - see front matter © 2011 Elsevier Ltd. All rights reserved.
doi:10.1016/j.ymssp.2011.11.008

first potential engineering application. Nowadays, MR fluids are commercially offered, especially by Lord Corp. and BASF Corp.

The experimental and theoretical studies reported in the present paper are focused on the application of MR fluid devices to the control of braking forces generated by industrial shock absorbers subjected to impact loading. The experimental results are compared with the predictions of a theoretical and simulation model.

2. Passive industrial shock absorbers

Typical shock absorbers are based on a hydraulic cylinder with a spring [1,4]. Fig. 1 shows two typical solutions. In the first solution the cylinder chambers are connected by a valve with orifices (Fig. 1a). In the second case there is a gap between the cylinder and the piston (Fig. 1b). When a load hits the shock absorber piston rod, the movement of the piston forces the hydraulic fluid to flow through orifices or gaps. These absorbers are quite well recognised and described in literature.

The paper [5] presents the state of the art in passive and active devices used in structural control systems. The first group encompasses a range of devices for enhancing structural damping, stiffness and strength. The second group includes active, hybrid and semi-active systems with controllable fluids. These systems use sensors, controllers and real-time information processing for control of damping forces. The cited paper includes an assessment of the state of the art and state of the practice of this exciting, and still evolving, technology.

Awrejcewicz et al. presented, in several publications, different aspects of theoretical, computational and experimental analysis of control of nonlinear dynamical systems with impacts. The overview of the most recent developments of such systems is presented in volume [6], which contains the invited papers presented at the Ninth International Conference "Dynamical Systems—Theory and Applications", held in 2007. One of those papers [7] investigates the dynamics of a material point moving in a gravitational field and colliding with a moving limiter. The authors sketched the overall picture of dynamic behaviour of the system, based on their analytical research and results of computations. They considered some very characteristic features of impacting systems, such as border-collisions and grazing impacts, which often lead to complex chaotic one-dimensional motion. Another paper [8] describes the transient in a nonlinear two-degrees-of-freedom system. It consists of a linear oscillator with a relatively big mass, which is an approximation of some continuous elastic system, and an essentially nonlinear absorber. Results of the simulation and analytical investigations of such system are presented. The impact dynamics control is also studied using delay feedback in [9,10]. A control of one- and two-degrees-of-freedom vibro-impact system with a delay is analysed there. The analytical approach to estimate the delay control coefficient is proposed and used for stabilisation of the system, composing and illustrating an effective control mechanism.

Real dynamic systems are always nonlinear. Therefore, there is a problem of how to measure existing forces and how to predict future impact forces that act in a nonlinear system. This problem is important in the control of damping of impact forces. E.g., a novel procedure to identify an impact load that acts on a nonlinear system is described in [11]. The problem of force prediction is solved by applying a stabilisation technique. In [12] a hydraulic damper is developed to generate a shock wave. The working principle of the damper is explained and the corresponding mathematical model is established. Paper [13] discusses the model identification of a continuously variable, electrohydraulic semi-active damper for a passenger car. A neural network is used to model the dynamic damper behaviour. The damper excitation signals are optimised. A validation of the proposed procedure shows that models identified from the data measured using the optimised excitations are considerably more accurate than those identified from data obtained using conventional random phase excitations. The article [14] discusses a new principle of active vibration control of flexible structural components with a controlled piezo-damper. Efficacy of the damper is demonstrated in mitigating vibration of a single-degree-of-freedom primary system. Effects of various parameters are studied to reveal the existence of optimum control parameters in controlling free vibration.

The braking force of a typical passive hydraulic shock absorber depends on the piston cross-section area, A_p and the pressure difference in piston chambers, Δp

$$F_b = A_p \Delta p. \tag{1}$$

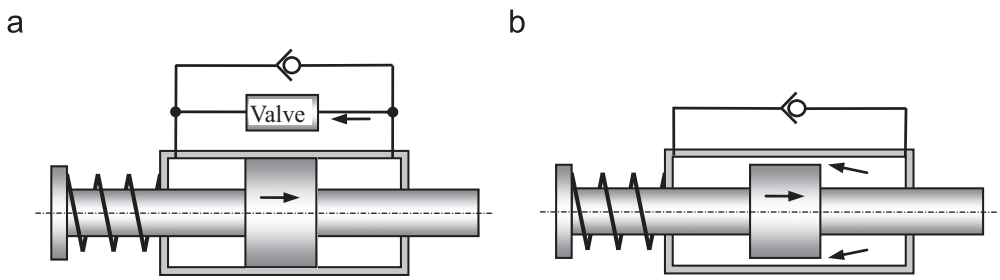

Fig. 1. Examples of typical hydraulic shock absorbers: (a) with a by-pass valve and (b) with an orifice between the piston and cylinder.

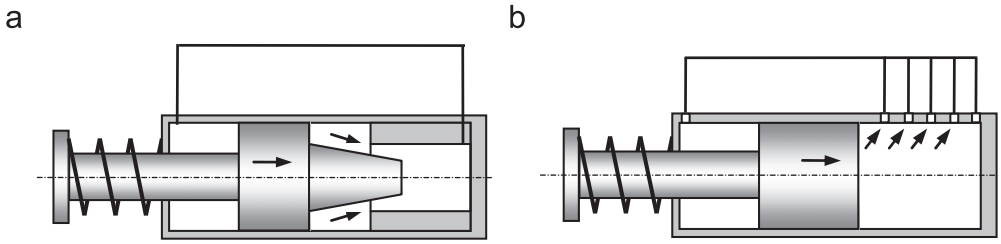

Fig. 2. Examples of hydraulic shock absorbers with orifices cross section area changing during movement.

From Bernoulli's equation we can obtain the following equation for fluid flow Q_a through a gap in a valve (also between cylinder chambers):

$$Q_a = A_p v_p = \alpha A_f \sqrt{\frac{2}{\rho}\Delta p} \tag{2}$$

where v_p—absorber piston speed during the stopping process, α—orifice discharge coefficient (0.3–0.6 for hydraulic oil), A_f—gap cross-section area, and ρ—fluid density.

Combining Eqs. (1) and (2) we obtain the braking force

$$F_b = \frac{A_p^3 \rho}{2\alpha^2 A_f^2} v_p^2. \tag{3}$$

This equation shows that the braking force is not constant and decreases proportionally to the square of piston velocity. At the beginning it is much higher than at the end, which means that the moving element is temporarily exposed to high deceleration. It is usually required that the moving element stops just before reaching the end of the absorber stroke. Therefore, when the velocity of the element changes; the braking force should be adjusted accordingly. To fulfil this requirement, the throttle orifice cross section area A_f should be changed according to the piston velocity or at least to the piston position.

In Fig. 2, examples of such adjustable absorbers are shown. The most commonly used type has several orifices along the cylinder (Fig. 2b). The orifices are closed one after the other when the piston moves. In this type of shock absorber, the braking force decreases proportionally to the square of piston velocity, but simultaneously increases stepwise, when consecutive orifices are closed. A model permitting the calculation of parameters of this shock absorber is given in [15]. Orifice areas and their positions are calculated using the equation of motion for an inertial load.

3. Industrial shock absorber with magnetorheological fluid

3.1. State of the art

Magnetorheological fluids were discovered and developed in the late 1940s. In the last 20 years many attempts have been made to apply MR fluids in dampers, brakes, clutches and other energy dissipating devices. An MR damper is one of the more promising devices used for oscillation reduction in structures. Such a damper is a semi-active control device which can generate a force according to applied electric current. The electrical energy required by such a damper is minuscule (a few Watts) while the dissipated energy can reach hundreds of Watts. The speed of its response is in the range of milliseconds. The results of research on the theory and application of MR fluids has been published in many papers [16–19]. For example, Wereley and Pang developed nonlinear quasi-steady ER and MR damper models using an idealised Bingham plastic shear flow mechanism [20]. The models are based on parallel plate or rectangular duct geometry, and are compared to 1D axisymmetric models.

Magnetorheological fluid is a suspension of ferromagnetic particles in a carrier liquid, usually mineral oil, synthetic oil, water or glycol. Ferromagnetic particles are soft iron particles, e.g. carbonyl iron (sometimes cobalt or nickel) with a diameter of 3–10 μm. The percentage of ferromagnetic particles in the liquid is usually in the range of 20–50% (max. 85%). Proprietary additives similar to those applied in commercial lubricants are commonly added to discourage gravitational settling and promote particle suspension, enhance lubricity, modify viscosity, and inhibit wear. Normally, MR fluids are free flowing liquids with a consistency similar to motor oil. However, in the presence of an applied magnetic field, the iron particles acquire a dipole moment aligned with the magnetic field, which causes particles to form linear chains parallel to the field. The fluid greatly increases its apparent viscosity, to the point of becoming a viscoelastic solid.

In the last few years, a number of MR fluid-based devices have been researched all over the world. One of the most popular applications is a semi-active suspension system [4,21,22] used in the automobile industry. Such systems are mass produced by Delphi Corp. (Delphi's MagneRide^{TM}). Examples of devices with the MR fluid include not only linear but also rotary dampers [18,23,24] and brakes [25]. Other potential applications include the absorption of shocks of off-road motorcycle systems [26] and seismic response reduction in buildings and bridges [16,18,23,27]. MR damper designs

typically place the coil in the piston head. In the design developed in the study [28] the coil is moved off the piston to either end of the damper. The active areas are stacked on both sides of the damper inner cylinder. The piston rides in this cylinder and forces fluid flow from one chamber through two bifold MR valves to the second chamber. Thus, four active volumes are created using only two coils. Two design goals are achieved: high force and compactness. The tests demonstrate that this novel MR damper was able to provide a high damping force at a high frequency (up to 12 Hz). Study [29] provides an experimental analysis of magnetorheological dampers subjected to impact and shock loading. A drop-tower is developed to apply impulse loads to the dampers. The results show that at large impact velocities, the peak force does not depend on the current supplied to the damper, as is commonly the case at low velocities. This phenomenon is hypothesised to be the result of the fluid inertia preventing the fluid from accelerating fast enough to accommodate the rapid piston displacement. Thus, the peak force is primarily attributed to compression of the MR fluid. The performance of ER and MR fluids under impulsively applied loads is also investigated in [2,30].

3.2. Approach discussed in detail

In order to have the possibility of controlling the braking force during the stopping process we propose an application of MR fluid in an industrial shock absorber (Fig. 3). The absorber proposed by us is based on a double rod hydraulic cylinder, in which chambers are connected by a by-pass cylindrical MR valve placed outside the cylinder. When the piston moves, the MR fluid flows from one chamber to the other through the MR valve. The effective fluid orifice is the entire annular space between the coil outside diameter and inside diameter of the valve housing. The design with a double-ended piston rod has an advantage: no rod volume compensator needs to be incorporated into the device.

A properly adjusted shock absorber should safely dissipate energy, reducing damaging shock loads and noise levels. At the beginning of the braking process, as shown in Fig. 4, the breaking force increases rapidly, due to the impact of the moving mass on the absorber piston rod, which is not moving [1]. The braking force then reduces gradually. As Fig. 4 illustrates, if the classical, passive shock absorber is used (curves 1, 2, 3), the force drops as the piston speed decreases. If the kinetic energy of the moving mass is too high, the mass is stopped by hard impact and bounces at the absorber bottom (curve 1). If this energy is too small, the mass is stopped before reaching the end position (curve 2). The proper matching of the braking force and the kinetic energy of the mass is shown by curve 3. For the case of using the MR fluid in the absorber, the force can be maintained at a more or less constant level, until the mass is stopped at the end position (curve 4). The value of the braking force is established by the electronic controller, which enables the adaptation of the braking force to the element kinetic energy. Summarising, we can hypothesise that the best stopping process can be obtained when using a shock absorber with MR fluid, proposed in this article.

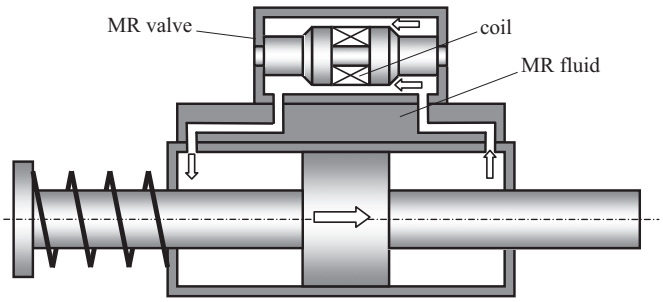

Fig. 3. Design of MR shock absorber.

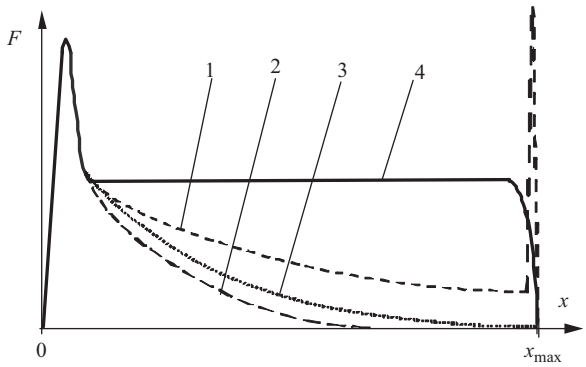

Fig. 4. Different braking characteristics (numbers explained in the text).

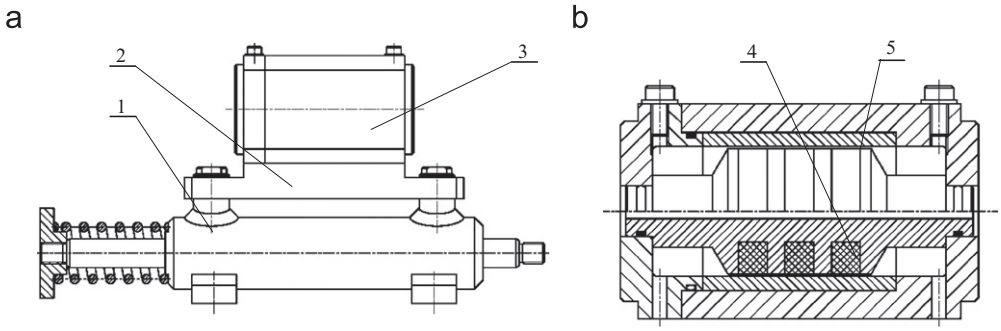

Fig. 5. Diagram of shock absorber with MR fluid (a) and its by-pass valve; and (b) 1—cylinder, 2—connection plate, 3—valve, 4—coil, and 5—valve gap.

The MR fluid shock absorber investigated in this paper is shown in Fig. 5. A by-pass valve (3) with a cylindrical gap is mounted on the interface plate (2). The complete shock absorber is 310 mm long and contains approximately 0.05 dm^3 of MR fluid. The electromagnetic coils are wired in three sections in the valve. This creates four areas of magnetic field across the valve gap where the fluid flows. We assumed that the piston moves at a constant velocity and MR fluid flow is fully developed. In the quasi-static analysis used in the initial design phase of the shock absorber, we used a simple Bingham plasticity model to describe the MR fluid behaviour. This model is effective in describing the essential field-dependent fluid characteristic. Phillips [31] derived a quintic equation, which can govern the pressure gradient in the flow of a Bingham fluid. Gavin et al. [32] extended the idea, based on the simple parallel-plate model, for describing the force–velocity behaviour of cylinder dampers. Based on the parallel-plate model further developed by Spencer et al. [33], the total damper pressure drop may be decomposed into an uncontrollable pressure drop and a controllable pressure drop due to controllable yield stress. Thus the valve pressure drop is the sum of the viscous component and the magnetic field dependent component. It can be defined using the following equation [1,18,19,33]:

$$\Delta p = \Delta p_\mu + \Delta p_\tau = \frac{12\mu A_p l}{h^3 w} v_p + \frac{c l_\tau}{h} \tau_{MR} \tag{4}$$

where μ—dynamic viscosity (Pa s), A_p—piston cross section area (m^2), v_p—piston velocity, l—gap length, l_τ—gap where magnetic field exists, h—gap height, w—gap width, c—an empirical factor, which is a function of fluid velocity ($c=2.07 \div 3.07$) (−), v_p—absorber piston speed, and τ_{MR}—yield stress developed in response to the applied magnetic field.

In the quasi-static analysis the total braking force generated by the MR shock absorber is a sum of three forces (without spring)

$$F_b = F_\tau + F_\mu + F_f = \Delta p_\tau A_p + \Delta p_\mu A_p + F_f \tag{5}$$

where F_b—braking force, F_μ—viscous force, F_τ—MR fluid flow force, and F_f—friction force.

To maximise the effectiveness of the MR shock absorber, the controllable force should be as large as possible. To obtain it, a small gap size is required. On the other hand, a small gap size decreases the controllable range, because the viscous force increases much faster ($1/h^3$) with the gap magnitude increase than the MR controllable force ($1/h$). Therefore a compromise is necessary. We decided to use a typical hydraulic cylinder with a stroke (braking distance) of 70 mm, piston diameter of 25 mm and piston rod diameter of 18 mm. In our research we assumed that the dissipated kinetic energy may be in the range of 10–125 J. So, when assuming that during the stopping process the braking force is constant, the absorber should be able to generate forces in the range of 143–1786 N. The parameters of the shock absorber were as follows: $A_p=0.24\times10^{-3}$ m^2, $l=0.036$ m, $l_\tau=0.012$ m, $w=0.094$ m, $v=0$–1.0 m/s, $\tau_{MR}=50\ 000$ Pa, $\mu=0.4$ Pa s. During the investigations two gap heights h were used: 0.0005 m and 0.00025 m. The maximum force caused by the MR fluid for the first height ranges from 576 N ($c=2$) to 864 N ($c=3$) and for the second from 1152 N ($c=2$) to 1728 N ($c=3$). For the absolute viscosity of MR fluid equal to 0.4 Pa s the plastic viscous force can reach 864 N for $h=0.0005$ m and 6924 N for $h=0.00025$ m and $v_p=1$ m/s.

4. Simulation of shock absorber with magnetorheological fluid

Based on Eqs. (4) and (5) and assuming that the shear stress–voltage characteristic is linear, the MR fluid dependent force can be defined as

$$F_\tau = \frac{A_p c l_\tau}{h} \tau_{MR}(U) = k_H U \mathrm{sgn}(v_p) \tag{6}$$

where k_H—absorber gain coefficient (1/m), U—coil supply voltage, and sgn—"signum" function.

After incorporating the dynamic properties of forces and taking the Laplace transform, Eq. (6) can be rewritten as follows [4]:

$$F_\tau(s) = \frac{k_H e^{-sT_d}}{(T_e s+1)(T_m s+1)} U(s)\mathrm{sgn}[v_p(s)] \tag{7}$$

where T_d—MR particles formulation delay time (2–5 ms), T_m—MR fluid time constant (1–2 ms), and $T_e = L/R$—electrical time constant.

It should be noticed that the value of the k_H coefficient is not constant for all operating conditions because of saturation and hysteresis. The viscous force can be modelled according to the following equation:

$$F_\mu(s) = \frac{12\mu A_p^2 l}{h^3 w} v_p(s) = k_\mu v_p(s) \tag{8}$$

The friction force F_f consists of a static friction force F_{sf} and a dynamic friction force F_{df}. The first one depends on the type of absorber piston rod seals, and the second one changes proportionally to the piston velocity. The total friction force can be described by a Stribeck curve as follows:

$$F_f = F_{df} + F_{sf} = k_f v_p + \mathrm{sgn}[v_p] F_{tm} e^{-\beta|v_p|} \tag{9}$$

where k_f—dynamic friction gain coefficient between piston-cylinder and piston rod-damper housing surfaces, F_{tm}—static force for $v_p \approx 0$, and β—coefficient.

After substituting Eqs. (7)–(9) into Eq. (5), we obtained a theoretical model of the MR shock absorber with nonlinear friction characteristics (Stribeck). A complete simulation model, built in the Matlab-Simulink software environment, is presented in Fig. 6 [34]. The input signals are velocity v_p and coil control voltage U. The output signal is the damping force F_b. The input voltage signal is transmitted to the block "Coil", which models the dynamic properties of the coil electric circuit (first order system). The nonlinear characteristic $\tau_{MR} = f(i)$ is modelled by the saturation function. This characteristic is taken from the MR fluid catalogue [35] and put into the Matlab model as a "Look-up-Table" block. In this block, an "abs" function is also added, which makes sure that the output force is always positive, even when the voltage signal U is negative. The "sgn" function guarantees that the braking force F_b is equal to zero when the piston velocity is equal to zero.

Fig. 7 presents the MR fluid shock absorber step responses obtained by simulation. Applying a magnetic field to MR fluid causes ferromagnetic particles to align into chains. Formulation of these chains takes a few milliseconds which results in reaction time delay. The delay visible in Fig. 7 is most probably caused by the abovementioned phenomenon. The simulation investigations were focused on the reduction of the MR shock absorber reaction time. We tested models of different electronic supply units and the best results were obtained when the current source was used. In order to simulate the braking process of a moving mass, the mass dynamics model must be also included in the MR shock absorber model described above. The scheme of the whole system is shown in Fig. 8. It consists of two masses m_1 (moving mass) and m_2 (mass of the absorber piston and piston rod) connected to each other with a spring, characterised by coefficient k_1. This spring models the stiffness of the absorber piston rod. The spring characterised by coefficient k_2 represents the stiffness of the absorber's body and is active when the piston reaches the absorber's end position.

When the moving mass m_1 hits the static mass m_2 and then both masses move together, their movement is braked by the MR fluid flow resistance in the absorber, which produces the force F_b controlled by supply voltage U. The whole system is described by the following equations:

$$m_1\ddot{x}_1 = -k_1(x_1 - x_2) - b_m\dot{x}_1 - b_r|\dot{x}_1 - \dot{x}_2| + F \tag{10}$$

$$m_2\ddot{x}_2 = F_b(U, \dot{x}_2) + k_1(x_1 - x_2) - k_2 \cdot f(x_2) \tag{11}$$

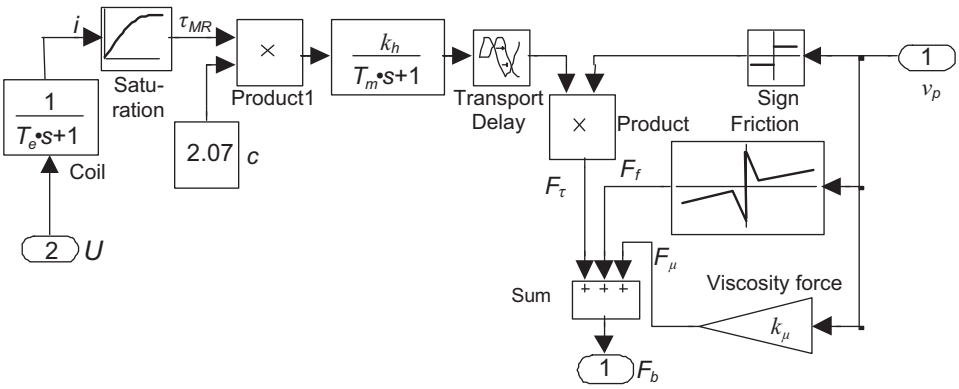

Fig. 6. Simulation model of the MR shock absorber.

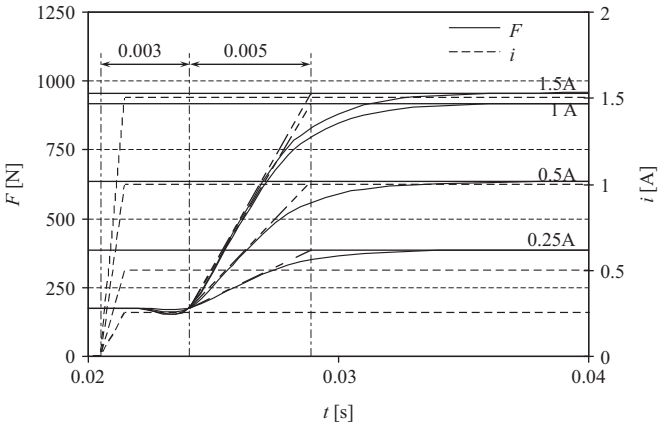

Fig. 7. Step responses of the shock absorber with the gap height equal to 0.5 mm (piston velocity 0.2 m/s).

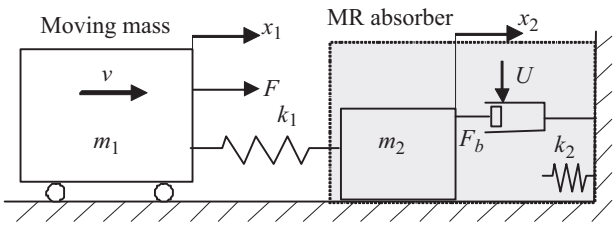

Fig. 8. Scheme diagram used for braking process dynamics modelling.

where m_1—moving mass, m_2—mass of piston and its rod, x_1, x_2—displacements of masses, k_1—piston rod stiffness, k_2—absorber body stiffness, F—gravity force acting on the mass on the inclined plane, b_m—viscous-friction coefficient, and b_r—equivalent of restitution coefficient.

We assumed that the collision of masses is only partially elastic, thus during the impact some of the energy is dissipated. In Eq. (10) the dissipating phenomenon is represented by an additional force which is proportional to the difference of both mass velocities. Thus, the dissipating process takes place only during the crash ($v_1 \neq v_2$).

The simulation model is presented in Fig. 9. It was prepared in Matlab-Simulink software. The MR shock absorber model shown in Fig. 6 was included in the model shown in Fig. 9. The Switch switches on the spring characterized by coefficient k_2 when the absorber piston reached the end position, modelling $f(k_2)$. In the simulation model presented here, a P-type position feedback controller was applied.

We assumed that the simulation begins when the collision begins; mass m_1 moves with velocity v_0 while mass m_2 is not yet moving. Before the start of every simulation the value of velocity v_0 was introduced into the integrative element called "$v1$" as the initial parameter. In order to model the impact of masses on the absorber edge, we assumed that the value of absorber body stiffness constant k_2 is equal to 0 when $x_2 < 70$ mm and increases stepwise up to 100 000 N/mm for $x_2 \geq 70$ mm. These changes in the value of coefficient k_2 were modelled by an "S-function" block in Matlab system.

Fig. 10 presents one example of simulation. Note that when the control is switched on (full-fine line), the braking force is almost constant and the bumps and bounces of masses against the absorber edge do not occur. On the contrary, when the process is not controlled, a strong bump occurs at the end of the movement.

5. Investigations of shock absorber with magnetorheological fluid

The MR fluid shock absorber described in this paper is shown in Fig. 11. A bypass valve (3) with a cylindrical gap was mounted on the interface plate (2). The complete shock absorber is approximately 310 mm long and contains approximately 0.05 dm^3 of the MR fluid.

Fig. 12 shows the block scheme of the experimental setup used for measuring the basic parameters of the MR shock absorber. An electrohydraulic servo drive was applied to control the velocity of the piston. The MR shock absorber and the drive were attached to a plate that was mounted on a strong floor. A Linear Variable Differential Transducer (LVDT) was used to measure the displacement (linearity 0.5%) and an HBM 5 kN transducer was used to measure the braking force. The measured signals (force and displacement) were transformed into a digital form by a 16-bit analogue/digital (ADC0 and ADC1) converter placed in an input/output card, and then sent to the computer and recorded in its memory. The displacement signal was differentiated in order to obtain the piston velocity. The same computer was used to control the electrohydraulic servo system velocity (DAC1) and the MR shock absorber coils current (DAC0). For the control, a 12-bit

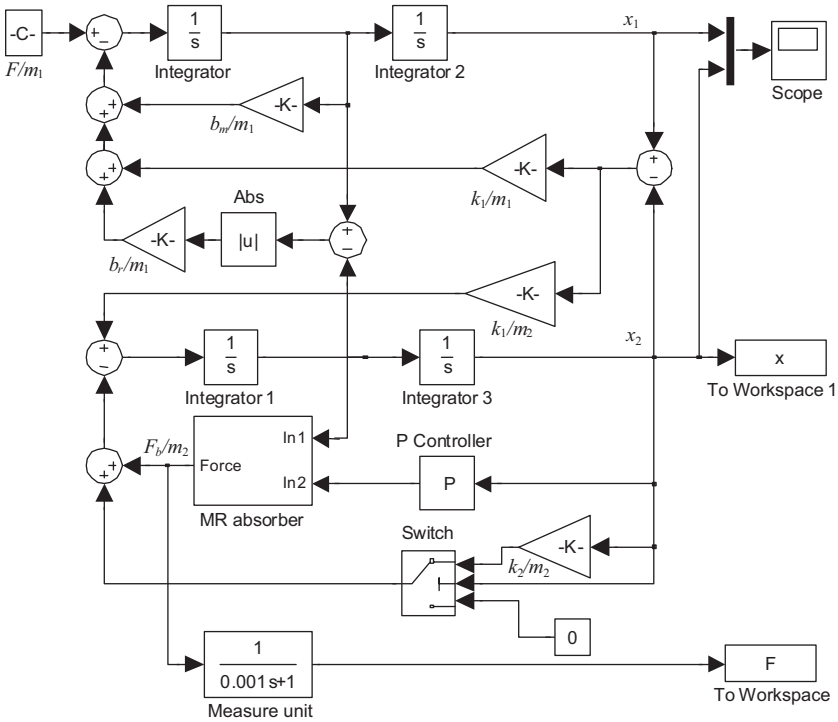

Fig. 9. Simulation model of the system for mass braking.

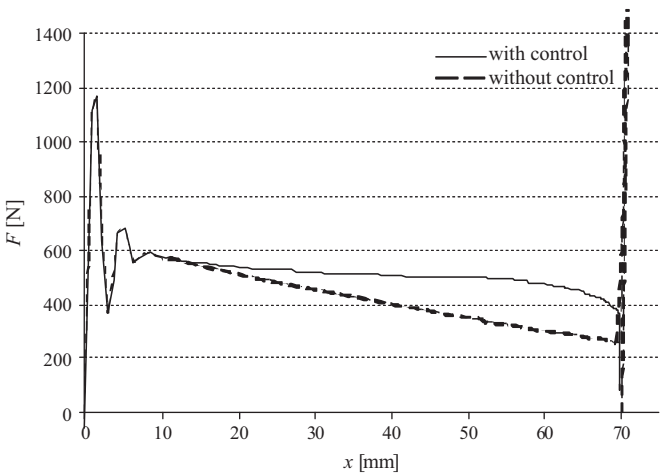

Fig. 10. Simulation results for $h=0.5$ mm, $E_k \approx 40$ J, initial velocity 0.35 m/s.

digital/analogue (d/a) converter was used. Digital outputs DO0 and DO1 were used to establish the coils current direction (the opposite direction was used for demagnetisation of the absorber magnetic circuit).

In this laboratory setup we investigated the braking force generated by the MR shock absorber for different coil currents and for different velocities of the MR absorber piston. The coils were supplied with current in the range of 0–1.2 A and the shock absorber piston velocity was increased linearly from 20 to 80 mm/s. The results are shown in Fig. 13a and b. The minimum force, caused only by flow resistance (viscous force at coil current of 0 A) and friction, for the gap height of 0.5 mm was approx. 200 N, and for the gap height of 0.25 mm approx. 400 N. One can note that the increase of force with velocity increase is much more significant when the gap height is 0.25 mm. For the valve gap height of 0.5 mm, the maximal force, generated by the absorber at coil current 1.0 A, was equal to approx. 900 N (Fig. 13a). When the gap height was equal to 0.25 mm, the maximal force was approximately two times bigger (2000 N) for similar coil current. The investigations have shown that for gap height 0.5 mm the influence of velocity is almost not visible. This is most probably

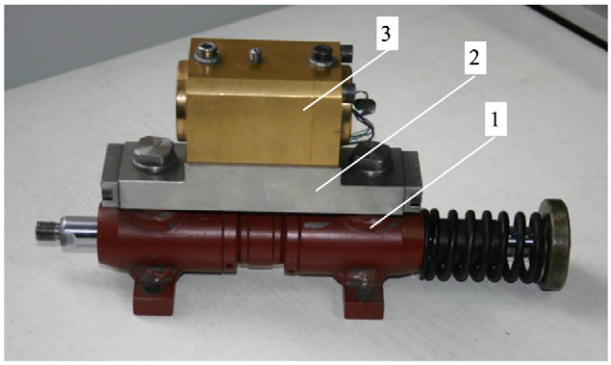

Fig. 11. Photo of MR shock absorber built during investigations.

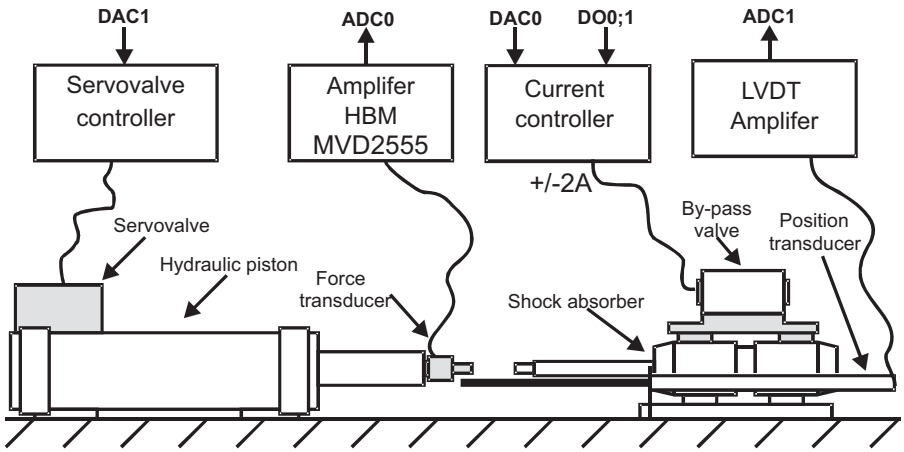

Fig. 12. Block scheme of experimental setup (DAC0; DAC1, ADC0; ADC1—computer analogue outputs and inputs, respectively, DO0;1—two digital outputs).

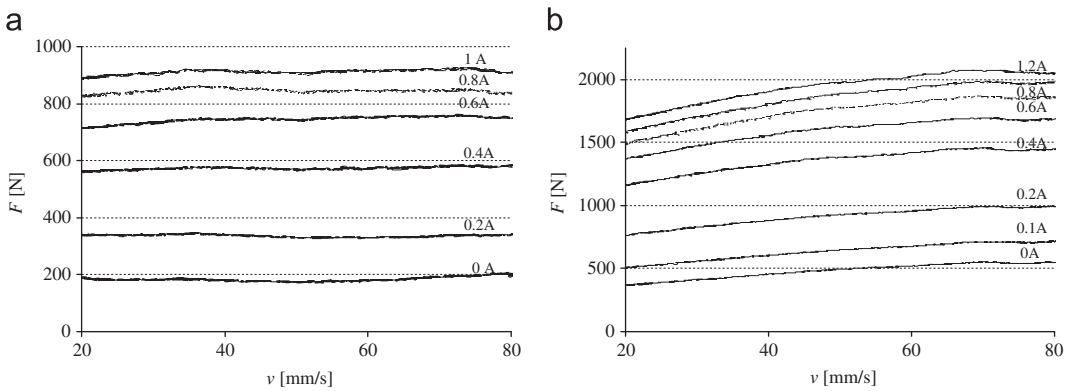

Fig. 13. Static characteristics of a built shock absorber with the gap height equal to: (a) 0.5 mm and (b) 0.25 mm.

because the viscous force is inversely proportional to the cubic of gap height, as shown in Eq. (3) and the increase of velocity has negligible influence on the total force.

The experimental setup was also used to record the MR shock absorber step responses for different coil currents, as shown in Fig. 14. In this investigation the shock absorber piston was moving, driven by an electrohydraulic servo system, with constant velocity of 0.09 m/s. During this movement the MR absorber coils were switched on stepwise. A specially designed electronic current source was used to supply the coils. The recorded curves show that the MR shock absorber is characterised by the delay equal to 4 ms for the gap height of 0.5 mm and equal to 3 ms for the gap height of 0.25 mm. The settling time ($0.9F_{max}$) was approx. equal to 5 ms and to 7 ms, respectively, so the whole reaction time was about 10 ms.

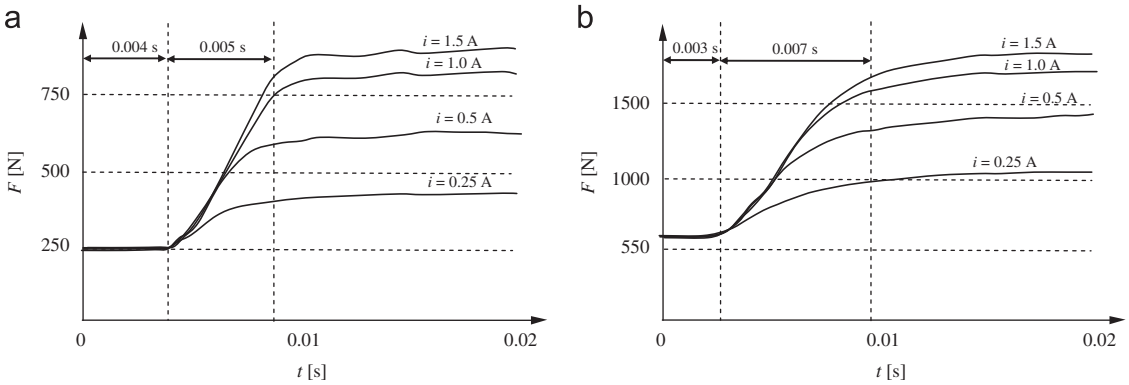

Fig. 14. Step responses of a built shock absorber with the gap height equal to: (a) 0.5 mm and (b) 0.25 mm (0.09 m/s).

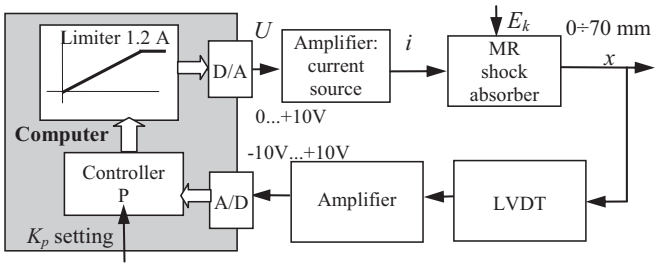

Fig. 15. Block diagram of piston position control.

Comparing the step responses obtained experimentally (Fig. 14a) with results obtained in simulation (Fig. 7) one can note that the reaction delay time of a real absorber is a bit longer than assumed in simulation model. The same issue concerns the not-controlled force which is about 250 N in the real absorber, while the in simulation model it is in the region of 200 N. Additionally, in real absorber, some nonlinear behaviour can be noted.

6. Control of shock absorber with magnetorheological fluid

As shown in Fig. 4, the most efficient way of stopping the elements moving on production lines is reached when the braking force is constant on the whole stopping distance. This, however, is not the case when we have to stop a bus or another vehicle with human beings onboard. Here, it seems that the braking force should be gently reduced before the final stop. In industrial applications there is an expectation that the element should be stopped just before the end point of the shock absorber. In order to obtain this, the braking force must be adapted to the element's initial kinetic energy ($F_b = E_k/x_{\max}$). This adaptation, for simple cases, can be done by a human operator just before stopping, after initial calculation confirmed by a few experiments.

In order to perform fully automated control of the MR shock absorber, its control system needs to calculate the moving mass kinetic energy. To this end we considered the application of piston displacement, its velocity, acceleration and braking force (pressure difference) as feedback signals for control. In practice, piston displacement is quite easy to measure, by applying a Linear Variable Differential Transducer, and this is why we focused on it during our investigations. However, the measurement of displacement is not sufficient to calculate the kinetic energy, and the control method proposed here does not provide full automation.

In a classical hydraulic shock absorber, during the stopping process the braking force decreases, which is caused by the decrease of the piston velocity. So, in the investigations presented here we applied only a control algorithm, which increases the MR shock absorber coil current linearly with the displacement changes of the piston, thus eliminating the decrease in force generated by the MR absorber.

The block scheme diagram of the system used for this control method is shown in Fig. 15. The heart of the system is a computer with A/D and D/A converters. The control program was implemented in C++ language. The control algorithm generated the coil control signal proportionally to the measured displacement. In this case, a P-type classical controller was used. In initial investigations its gain coefficient K_p was calculated by a human operator off-line and entered into the control program every time the mass energy was changed. Based on Eqs. (4) and (5), the simplified equation for the shock absorber braking force F_b calculation can be written as follows:

$$F_b = F_{fs} + k_f v_p + k_\mu v_p + k_H U \operatorname{sgn} v_p \approx F_{fs} + k_{\mu f} v_p + k_\tau \sqrt{i} \operatorname{sgn} v_p \tag{12}$$

where F_{fs}—static friction force, k_f—friction coefficient, k_μ—viscosity coefficient, k_τ—MR fluid coefficient, and $k_{\mu f}=k_\mu+k_f$—movement resistance coefficient.

In this equation the MR fluid force is a function of the square root of coil current, which simplifies (approximates) the saturation of the magnetic field and the MR fluid (see MR fluid characteristic $\tau=f(H)$ in [35]). We estimated the parameters in Eq. (12) taking into account the investigation results presented in Figs. 13 and 14. The parameters of friction force (see Fig. 13) were estimated as follows: $F_{fs}=250$ N and $k_{\mu f}=830$ N s/m (force increase of approx. 50 N caused by velocity increase of 0.06 m/s) for gap height 0.5 mm; and $F_{fs}=400$ N and $k_{\mu f}=7500$ N s/m (force increase of approx. 450 N caused by velocity increase of 0.06 m/s) for gap height 0.25. Based on Eq. (8), the viscosity coefficient k_μ was calculated as approx. 850 N s/m for a gap height of 0.5 mm and as 6590 N s/m for a gap height of 0.25 mm. These values are almost the same as estimated above for coefficient $k_{\mu f}$, which means that the value of friction coefficient is almost equal to 0 N s/m. We substituted the values of current and force taken from curves presented in Fig. 14 into equation $F=k_\tau\sqrt{i}$ and approximated the MR fluid coefficient k_τ as $500\,\mathrm{N}/\sqrt{\mathrm{A}}$ for gap height 0.5 mm and as $1000\,\mathrm{N}/\sqrt{\mathrm{A}}$ for gap height 0.25 mm. As mentioned above, we decided to use a control algorithm in which the absorber controller increased the coil current in the function of the measured piston displacement $x=x_2$. So, the value of the coil current was calculated by the controller according to the equation $i=K_p \ldots x$. Taking into account that the moving mass kinetic energy E_k should be dissipated on the shock absorber displacement distance ($x_{\max}=0.07$ m) and that the braking force is constant, the appropriate control equation for proper stopping process is

$$E_k=F_b x_{\max}=(F_{fs}+k_f v_p+k_\mu v_p+k_\tau\sqrt{K_p x})x_{\max} \tag{13}$$

The equation used for calculation of controller gain coefficient K_p was established based on Eq. (13), in which x was taken as $x_{\max}$ and v_p as an average value of velocity ($v_p=v_s/2$).

$$K_p=\frac{(E_k-(F_{fs}+k_f v_p+k_\mu v_p)x_{\max})^2}{k_\tau^2 x_{\max}^3} \tag{14}$$

In our investigations the value of gain coefficient K_p was in a range from 2 A/m to 15 A/m, according to moving mass kinetic energy and absorber valve gap height.

Fig. 16 shows the scheme of the second experimental setup we used in the investigations. It was arranged on an inclined plane with an angle that could be changed in the range of 0–20°. This stand was used to test the efficacy of the MR shock absorber and its control methods. The MR shock absorber piston displacement and forces generated during the braking process were measured and recorded by a computer with an input/output card.

Before each test, the mass (wagon) of 88 kg or 134 kg was lifted to a height in the range of 13 mm to 60 mm, and the mass velocity v_s at the point in which the stopping process began ranged from 0.5 m/s to almost 1.0 m/s. After releasing the wagon, it was accelerated by gravity force and hit the MR shock absorber piston rod at the end of inclined plane. The kinetic energy of the moving mass was in the range of 11 J to about 125 J.

The results of experimental investigations obtained when using the controller described above are shown in Fig. 17 for gap heights of 0.5 mm and 0.25 mm. The curves presented in Fig. 17 show that the time of the stopping process was about 0.15 s when there was no control and about 0.22 s when the controller was switched on. One can note that when the stopping process was not controlled, the forces decrease during the stopping process, and at the end of the movement the piston bounces on the cylinder bottom. This is evident from Fig. 17, where several impacts and bounces can be observed.

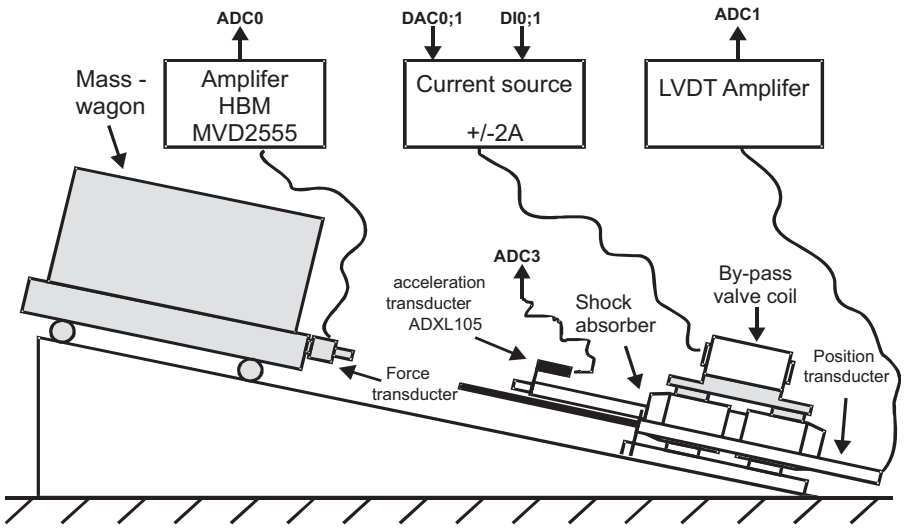

Fig. 16. Block schemes of experimental setup (DAC0; DAC1, ADC0; ADC1; ADC3—analogue outputs and inputs, respectively, DO0; DO1—digital outputs).

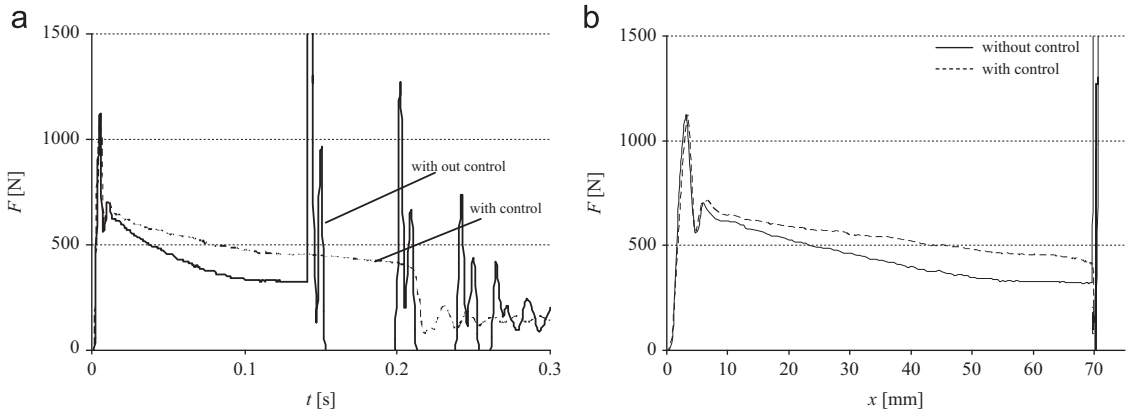

Fig. 17. Force curves during stopping process for $h=0.5$ mm, $E_k \approx 45$ J, initial velocity $v_s=0.35$ m/s, $K_p=4$ A/m in function of: (a) time and (b) displacement.

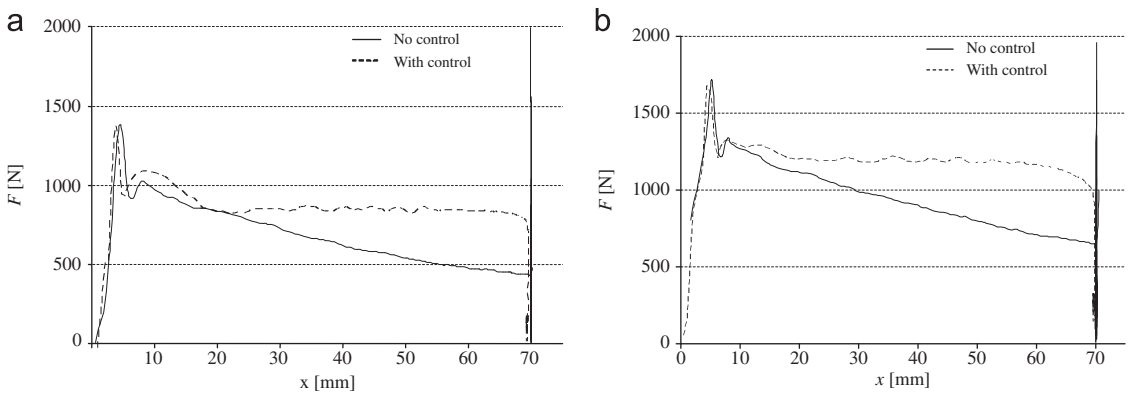

Fig. 18. Force curves during stopping process for: (a) $h=0.5$, $E_k \approx 60$ J, initial velocity $v_s=0.45$ m/s; (b) $h=0.25$, $E_k \approx 90$ J, initial velocity $v_s=0.60$ m/s.

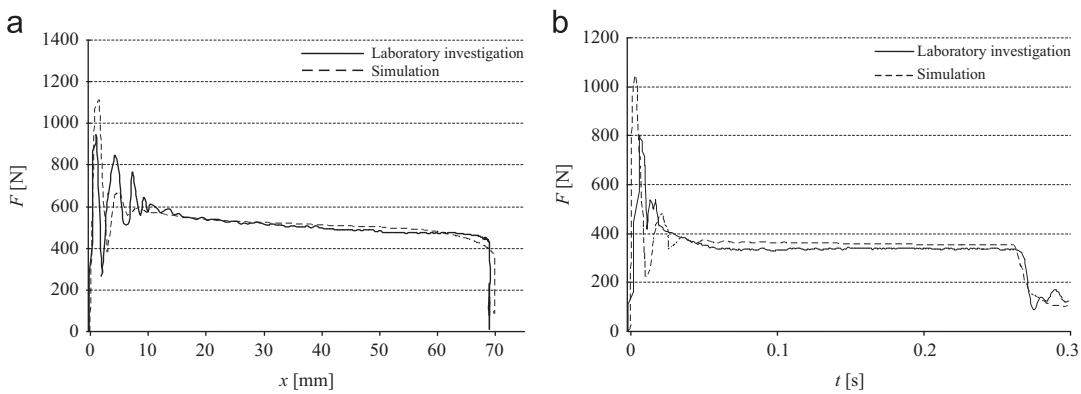

Fig. 19. Force curves during stopping process for: (a) coil current proportional to the position; $h=0.5$, $E_k=40$ J, initial velocity $v_s=0.35$ m/s and (b) coil current proportional to square of the position; $h=0.5$, $E_k=30$ J, initial velocity $v_s=0.30$ m/s.

However, even if the controller is switched on, the braking force still decreases during the stopping process. This is why we decided to change the control algorithm into a nonlinear one in which the current was calculated according to the equation $i=K_{p1} \ldots x^2$. The results of experimental investigations obtained when using this controller are shown in Fig. 18. When the controller is switched on, the force curves are almost flat, and thus the braking process is close to ideal.

The accuracy of the simulation model was validated in two-step investigations: first, in simulations, and then in a laboratory environment as well. Examples of the results are shown in Fig. 19. One can note that with exception of the bumping phase, the results obtained by the simulations are very close to the results obtained in the laboratory investigations.

7. Conclusions

In the paper the theoretical and simulation model of an MR shock absorber, as well as the complete stopping model, is presented. The design and investigation results of a real MR absorber and its controller are shown. The comparison of results obtained by simulation and laboratory investigations has confirmed that the simulation model corresponds well with the real MR absorber. The investigations have proved that the use of MR fluid in industrial shock absorbers enables an electronic control circuit to match the braking characteristic to the stoppable mass kinetic energy. The MR shock absorbers can be built in the control loop of modern fully automated production lines, in which different elements are moved with different energy in the same time. The investigations have confirmed the positive influence of control methods on the braking process. Empirical tests demonstrated that when the adjustment of stopping control process parameter (gain coefficient) is set correctly, the braking process is similar to uniformly retarded. The investigations have shown that the use of a simple P-type controller was sufficient to perform the task described in this paper.

The main disadvantage of the presented control method is the necessity to establish a proper value of gain coefficient, which must be calculated according to Eq. (7) and introduced manually before the braking process. If the controller parameters were calculated and introduced properly, the moving element was stopped just before reaching the absorber bottom and impact did not occur.

In our further investigations we are going to apply other sensors and control methods, which will enable the automatic calculation or estimation of the moving mass kinetic energy at the beginning of the braking process. This will enable on-line calculation of the value of the braking force F_b. In order to solve this problem, an additional algorithm should be worked out and implemented. We are also considering the usage of a cheap acceleration transducer to improve the calculations.

The main advantage of using MR fluids in industrial shock absorbers is the possibility to set and control their braking parameters. The mechanical simplicity, high dynamic range, low power requirements, large force capacity and robustness of magnetorheological fluid industrial shock absorbers match well with application demands and constraints, offering an attractive means of protecting automated lines against sudden impact of movable elements.

Acknowledgements

The work described in this paper was supported by Polish Ministry of Science and Education in the years 2009 to 2012 as a Grant no. N502 260737.

References

[1] M. Hauke, Basic Theory and Investigation of Industrial Hydraulic Shock Absorbers with Magnethoreological Fluids, (in Polish) Ph.D. Thesis, Poznań University of Technology, 2006.
[2] A.K. El Wahed, J.L. Sproston, G.K. Schleyer, A comparison between electrorheological and magnetorheological fluids subjected to impulsive loads, in: Proceedings of the Seventh International Conference on Electrorheological (ER) Fluids and Magneto-Rheological (MR) Suspensions. Honolulu, Hawaii, 1998, pp. 401–410.
[3] W. Winslow, Electrorheological coupling, Journal Applied Physics 20 (1949).
[4] J.C. Dixon, The Shock Absorber Handbook, SAE International and John Wiley & Sons, Ltd., 2007.
[5] T.T. Soong, B.F. Spencer Jr., Supplemental energy dissipation: state-of-the-art and state-of-the practice, Engineering Structures 24 (2002) 243–259.
[6] J. Awrejcewicz, (Editor), Modeling, Simulation and Control of Nonlinear Engineering Dynamical Systems: State of the Art, Perspectives and Applications, Springer-Verlag, 2009.
[7] A. Okninski, B. Radziszewski, Analytical and numerical investigations of impacting systems: a material point colliding with a limiter moving with piecewise constant velocity, in: Modeling, Simulation and Control of Nonlinear Engineering Dynamical Systems: State of the Art, Perspectives and Applications, Springer-Verlag, 2009.
[8] Yu.V. Mikhlin, G.V. Rudneva, T.V. Bunkova, Transient in 2-dof system which contains an essentially nonlinear absorber, IN: Modeling, Simulation and Control of Nonlinear Engineering Dynamical Systems: State of the Art, Perspectives and Applications, Springer-Verlag, 2009.
[9] J. Awrejcewicz, K. Tomczak, Stability improvement of the vibro-impact discrete systems, EUROMECH Colloquium, in: V.I. Babitsky (Ed.), Dynamics of Vibro-Impact Systems, 1998, Springer-Verlag, Berlin, Heidelberg, 1999, pp. 109–118.
[10] J. Awrejcewicz, K. Tomczak, C.-H. Lamarque, Controlling system with impacts, International Journal of Bifurcation and Chaos 9 (3) (1999) 547–553.
[11] T.S. Janga, B. Hyoungsu, S.L. Hana, T. Kinoshitac, Indirect measurement of the impulsive load to a nonlinear system from dynamic responses: Inverse problem formulation, Mechanical Systems and Signal Processing 24 (6) (2010) 1605–1920.
[12] S. Jiao, Y. Wang, L. Zhang, H. Hua, Shock wave characteristics of a hydraulic damper for shock test machine, Mechanical Systems and Signal Processing 23 (5) (2010) 1605–1920.
[13] M. Witters, J. Swevers, Black-box model identification for a continuously variable, electro-hydraulic semi-active damper, Mechanical Systems and Signal Processing 24 (1) (2010) 4–18.
[14] S. Chatterjee, On the principle of impulse damper: A concept derived from impact damper, Journal of Sound and Vibration 312 (2008) 584–605.
[15] A.K. Smirnov, On dynamic synthesis of a hydraulic shock absorber with discrete disposition of throttling windows, Journal of Machinery Manufacture and Reliability 37 (4) (2008) 330–339.
[16] M.R. Jolly, J.W. Bender, J.D. Carlson, Properties and Applications of Commercial Magnetorheological Fluids, in: Proceedings of the Fifth SPIE annual international symposium on smart structures and materials, San Diego, CA, 1998.
[17] P. Phule, Magnetorheological (MR) fluids: principles and applications, Smart Materials Bulletin (2001) 7–10.
[18] G. Yang, Large Scale Magnetoreological Fluid Damper for Vibration, Ph.D. Thesis, Department of Civil Engineering and Geological Science, Notre Dame, Indiana, 2001.
[19] R.W. Philips, Engineering Applications of Fluids with a Variable Yield Stress, Ph.D. Thesis, University of California, Berkeley, 1969.
[20] N.M. Wereley, L. Pang, Nondimensional analysis of semiactive electrorheological and magnetorheological dampers using approximate parallel plate models, Smart Material Structures 7 (5) (1998) 732–743.

[21] S.B. Choi, M.H. Nam, B.K. Lee, Vibration control of a MR seat damper for commercial vehicles, Journal of Intelligent Material Systems and Structures 12 (2000) 936–944.
[22] A. Milecki, M. Hauke, D. Sedziak, J. Ortmann, Controllability of MR shock absorber for vehicle, International Journal of Vehicle Design 38 (2/3) (2005) 222–233.
[23] S.J. Dyke, B.F. Spencer, M.K. Sain, J.D. Carlson, Modeling and control of magnetorheological dampers for seismic response reduction, Smart Material Structure 5 (1996) 565–575.
[24] S.R. Hong, S.B. Choi, Y.T. Choi, N.M. Wereley, Non-dimensional analysis and design of a magnetorheological damper, Journal of Sound and Vibration 288 (4–5) (2005) 847–863.
[25] J. Huang, J.Q. Zhang, Y. Yang, Y.Q. Wei, Analysis and design of a cylindrical magneto-rheological fluid brake, Journal of Materials Processing Technology 129 (2002) 559–562.
[26] E.O. Eriksen, F. Gordaninejad, A magneto-rheological fluid shock absorber for an off-road motorcycle, International Journal of Vehicle Design 33 (1–3) (2003) 139–152.
[27] Z. Akaby, H.M. Aktan, Intelligent energy dissipation devices, in: Proceedings of the Fourth US National Conference on Earthquake Engineering, vol. 3, Palm Springs, 1990, pp. 427–435.
[28] W.B. Facey, N.C. Rosenfeld, Y.T. Choi, N.M. Wereley, S.B. Choi, P.C. Chen, Design and testing of a compact magnetorheological damper for high impulsive loads, International Journal of Modern Physics B 19 (7–9) (2005) 1549–1555.
[29] M. Ahmadian, A.N. James, Experimental analysis of magnetorheological dampers when subjected to impact and shock loading, Communications in Nonlinear Science and Numerical Simulation 13 (2008) 1978–1985.
[30] A.K. El Wahed, J.L. Sproston, G.K. Schleyer, Electrorheological and magnetorheological fluids in blast resistant design applications, Materials and Design 23 (2002) 391–404.
[31] R.W. Philips, Engineering Applications of Fluids with Variable Yield Stress, Ph.D. Thesis, University of California, Berkley, 1996.
[32] G.P. Gavin, R.D. Hanson, F.E. Filisko, Electrorheological dampers. Part I and II, Journal of Applied Mechanics ASME 63 (9) (1996) 669–682.
[33] B.F. Spencer Jr., G. Yang, J.D. Carlson, M.K. Sain, 'Smart' dampers for seismic protection of structures: a full-scale study, in: Proceedings of the Second World Conference on Structural Control, vol. 1, Japan, 1998, pp. 417–426.
[34] A. Milecki, Modeling of magneto-rheological shock absorbers, Archives of Mechanical Technology and Automation 24 (2) (2004) 123–129.
[35] 〈http://www.lord.com〉, 〈http://www.lordfulfillment.com/upload/DS7012.pdf〉.